Analytical integration of the Green's tensor in the discrete dipole approximation

Maxim A. Yurkin[1] and Dmitry A. Smunev[2]

[1]*Novosibirsk State University, Pirogova 2, 630090 Novosibirsk, Russia*
[2]*Warsaw, Poland*

While historically the discrete dipole approximation (DDA) implied the interaction of point dipoles, integration of the corresponding free-space Green's tensor (IGT) over the cuboid voxel is known to improve the performance of the method. Previous implementations used either slow numerical integration or some approximations with poorly controlled errors. We present the analytical IGT over arbitrary cuboid voxel, neglecting only the terms of fourth order of kd (voxel size parameter), and implement it in the open-source code ADDA. This implementation is much faster than numerical integration, while guaranteeing excellent accuracy for any input parameters. The improved IGT formulation leads to quadratic convergence in terms of kd for cubes and allows robust simulation of interaction of internal sources with particles of arbitrary shapes.

INTRODUCTION

The discrete dipole approximation (DDA) is a general method to simulate light scattering by particles of arbitrary shape and internal structure [1]. While the method is commonly associated with a physically clear picture of interacting point dipoles, there exist modern DDA formulations departing from this picture. One of such formulations is the integration of Green's tensor (IGT) [2], which naturally follows from the rigorous derivation of the DDA through the discretization of the volume integral equation [1]. Apart from being more mathematically justified, the IGT is known to solve the convergence problems of the standard (point-dipole) DDA for high-contrast dielectric nanoparticles (large real refractive index m) [3,4]. Moreover, the IGT is critical for the successful usage of rectangular-cuboid discretization voxels [3], and should lead to quadratic convergence (in terms of voxel size d) for shapes exactly described by a set of cubes [5].

As follows from its name, IGT incurs integration over the voxel (generally, a cuboid). This can be done numerically but can take considerable computational time due to oscillating nature of the integrand. That is not a bid deal for volume-integral codes based on matrix inversion, such as pyGDM [6], but may take a large fraction of the total simulation time for conventional DDA codes, based on the FFT-accelerated iterative solution. In particular, IGT with numerical evaluation of integrals has been implemented in the ADDA code long ago [7], but its use was mostly accompanied by some approximations. Either the IGT was used only for two points closer than a certain threshold (say, $3d$) or an approximation was used based on tabulated values of auxiliary integrals (only for cubical voxels) [8]. Both these options have favorable convergence of the iterative solver, but the remaining error due to the used approximations is poorly known. While the latter is sufficiently small for a wide majority of practical applications,

it hampers sensitive convergence studies, e.g., for numerical tests of the abovementioned quadratic convergence. The same problem applies to the fully-numerical IGT as well, since it uses a built-in threshold.

While fully analytic integration of the Green's tensor does not seems feasible, in this work we perform such integration keeping the error $\mathcal{O}[(kd)^4]$, where k is the wavenumber. This is sufficient for *all* purposes, since the error of the DDA itself (using any formulation) is $\mathcal{O}[(kd)^2]$ or larger [5]. We further implement the developed formulae in the ADDA code and numerically verify the quadratic convergence with respect to d. Finally, we discuss other potential applications of the IGT.

INTEGRATION OF THE STATIC PART

The free-space Green's tensor is given as:

$$\bar{\mathbf{G}}(\mathbf{r}) = \frac{\exp(\mathrm{i}kr)}{4\pi r}\left[\left(\bar{\mathbf{I}} - \frac{\mathbf{r}\otimes\mathbf{r}}{r^2}\right) + \frac{\mathrm{i}kr-1}{k^2r^2}\left(\bar{\mathbf{I}} - 3\frac{\mathbf{r}\otimes\mathbf{r}}{r^2}\right)\right], \tag{1}$$

where $\mathbf{r}$ is generally a distance between two points, $r = |\mathbf{r}|$, and $\mathbf{r}\otimes\mathbf{r}$ is a dyad defined as: $(\mathbf{r}\otimes\mathbf{r})_{\mu\nu} = \mathbf{r}_\mu\mathbf{r}_\nu$ (μ and ν – are Cartesian components of the tensor or vector), $\bar{\mathbf{I}}$ is an identity matrix, and $\exp(-\mathrm{i}\omega t)$ time dependence of harmonic fields is assumed. The static limit is given as

$$\begin{gathered}\bar{\mathbf{G}}(\mathbf{r}) \underset{kR\to 0}{\longrightarrow} \bar{\mathbf{G}}_{\mathrm{st}}(\mathbf{r}) + \mathcal{O}(1/r),\\ \bar{\mathbf{G}}_{\mathrm{st}}(\mathbf{r}) = (\nabla\otimes\nabla)\frac{1}{4\pi k^2 r} = -\frac{1}{4\pi k^2 r^3}\left(\bar{\mathbf{I}} - 3\frac{\mathbf{r}\otimes\mathbf{r}}{r^2}\right).\end{gathered} \tag{2}$$

The direct consequence of the aimed order of errors is that we need to perform integration *exactly* for small scatterer, which requires analytic integration of $\bar{\mathbf{G}}_{\mathrm{st}}(\mathbf{r})$. Fortunately, this can be accomplished using the third antiderivative (can be verified by differentiation):

$$\bar{\mathbf{F}}(\mathbf{r}) \overset{\text{def}}{=} -4\pi k^2 \iiint \mathrm{d}x\mathrm{d}y\mathrm{d}z\, \bar{\mathbf{G}}_{\mathrm{st}}(\mathbf{r}), \qquad F_{\mu\nu}(\mathbf{r}) = \begin{cases} \arctan\dfrac{V_{\mathbf{r}}}{r_\mu^2 r}, & \mu = \nu, \\ -\operatorname{artanh}\dfrac{V_{\mathbf{r}}}{r_\mu r_\nu r}, & \mu \neq \nu, \end{cases} \tag{3}$$

where x, y, z are the Cartesian components of $\mathbf{r}$, $V_{\mathbf{r}} \overset{\text{def}}{=} xyz$ (can be negative, but assumed to be non-zero), and $\operatorname{artanh} x = (1/2)\ln[(1+x)/(1-x)]$ is the inverse hyperbolic tangent. Thus, the integral of $\bar{\mathbf{G}}_{\mathrm{st}}(\mathbf{r})$ over any cuboid (aligned with the coordinate axes) is proportional to a triple difference of values of $\bar{\mathbf{F}}(\mathbf{r})$ at its vertices. This is valid even for cuboids enclosing the origin, if the corresponding singular integral is considered as a surface one (so-called L-term).

INTEGRATION OF THE DYNAMIC PART

To proceed beyond the static limit, we continue the expansion of $\overline{\mathbf{G}}(\mathbf{r})$ in series of kr, by introducing (see, e.g., Eq. (A3) of [9]):

$$\overline{\mathbf{A}}(\mathbf{r}) \stackrel{\text{def}}{=} 4\pi k^2[\overline{\mathbf{G}}(\mathbf{r}) - \overline{\mathbf{G}}_{\text{st}}(\mathbf{r}) - \overline{\mathbf{G}}_1(\mathbf{r})] = \frac{2}{3}\mathrm{i}k^3\bar{\mathbf{I}} + \mathcal{O}(k^4 r), \tag{4}$$

$$\overline{\mathbf{G}}_1(\mathbf{r}) \stackrel{\text{def}}{=} \frac{1}{8\pi r}\left(\bar{\mathbf{I}} + \frac{\mathbf{r}\otimes\mathbf{r}}{r^2}\right), \tag{5}$$

Importantly, the series for $\overline{\mathbf{G}}(\mathbf{r})$ have infinite radius of convergence (due to exponents), and, hence, can be differentiated term-wise. Similarly to Eq. (3), there exist an analytic third anti-derivative of $\overline{\mathbf{G}}_1(\mathbf{r})$:

$$\overline{\mathbf{B}}(\mathbf{r}) \stackrel{\text{def}}{=} 8\pi \iiint \mathrm{d}x\mathrm{d}y\mathrm{d}z\, \overline{\mathbf{G}}_1(\mathbf{r}),$$
$$B_{\mu\nu} = \begin{cases} \sum_\tau \left[\left(1+\delta_{\tau\mu}\right)\frac{V_\mathbf{r}}{r_\tau}\operatorname{artanh}\frac{r_\tau}{r} - \left(1-\delta_{\tau\mu}\right)r_\tau^2 \arctan\frac{V_\mathbf{r}}{r_\tau^2 r}\right], & \mu = \nu, \\ -\frac{1}{2}\left[\frac{V_\mathbf{r} r}{r_\mu r_\nu} + \left(r_\mu^2 + r_\nu^2\right)\operatorname{artanh}\frac{V_\mathbf{r}}{r_\mu r_\nu r}\right], & \mu \neq \nu. \end{cases} \tag{6}$$

The final component is the integration of $\overline{\mathbf{A}}(\mathbf{r})$, which is performed using its regularity at the origin, in contrast to extracted $\overline{\mathbf{G}}_1(\mathbf{r})$ and $\overline{\mathbf{G}}_{\text{st}}(\mathbf{r})$. A straightforward Taylor expansion leads to

$$\int_{V_\mathrm{d}} \mathrm{d}^3\mathbf{r}'\overline{\mathbf{A}}(\mathbf{R}) = V_\mathrm{d}\left\{\overline{\mathbf{A}}(\mathbf{r}) + \frac{1}{24}\mathcal{U}[\overline{\mathbf{A}}(\mathbf{r})] + \mathcal{O}\left[(kd)^4\frac{1+(kr)^2}{r^3}\right]\right\}, \tag{7}$$

$$\mathcal{U}[f(\mathbf{r})] \stackrel{\text{def}}{=} \sum\nolimits_\mu d_\mu^2 \frac{\partial^2 f(\mathbf{r})}{\partial r_\mu^2} \underset{\text{cub}}{=} d^2\nabla^2 f(\mathbf{r}), \tag{8}$$

where V_d is the cuboid voxel (dipole) centered at $\mathbf{r}$, while the last equality ("cub") is for a cubical one. The obtained remaining error is sufficient ($\mathcal{O}[(kd)^4]$) for $r \gtrsim d$, while omitting $\mathcal{U}[f(\mathbf{r})]$ leads to the same order of errors for smaller r.

Moreover, the above evaluation is redundantly complicated for $kr \gtrsim 1$ and may even lose significant digits due to the cancellation of some terms. In this case, the best option is to apply Taylor-expansion based formula [Eq. (7)] directly to $\overline{\mathbf{G}}(\mathbf{r})$, which has already been used in ADDA [8]. However, the specific optimal thresholds of r to switch between the described evaluation algorithms still need to be determined.

SIMULATION RESULTS

We have implemented the above formulae in ADDA and performed convergence studies for cubes with $m = 1.6 + 0.01\mathrm{i}$, $0.1 + \mathrm{i}$, $10 + 10\mathrm{i}$ and two sizes $kD = 8$ and 0.1 (comparable to and much smaller than the wavelength. The same cubes were considered in [10,11], where the reference values for efficiencies were obtained through the simulation with n_x (number of voxels along the cube edge) up to 512. We compared the extinction and absorption efficiencies

(Q_{ext} and Q_{abs}), computed with the analytic IGT and n_x up to 128, with this reference. The relative errors (REs) for a single case ($m = 1.6 + 0.01\mathrm{i}$, $kD = 8$), are shown in Fig. 1. It features close-to-quadratic convergence in contrast to the linear one, observed previously for point-dipole formulations of the DDA [10]. The results for other cases and with larger n_x will be shown at the conference.

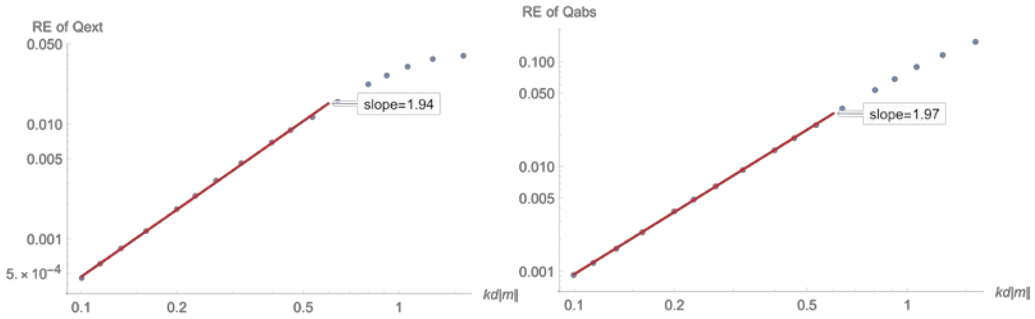

Fig. 1. Relative errors of Q_{ext} and Q_{abs}, computed with the IGT, versus the discretization parameter (in log-log scale) for a cube with $kD = 8$ and $m = 1.6 + 0.01\mathrm{i}$. Also shown are the linear fits through the points with $kd|m| \leq 0.5$.

Another relatively novel application of the DDA is when the incident field is generated by a point source placed inside the particle, which is relevant, e.g., for near-field radiative heat transfer [12]. If such source is naively used in the point-dipole DDA, the result is highly sensitive to its position with respect to the voxel lattice [13]. By contrast, the IGT is free of these deficiencies, if the incident field is computed not in the center, but averaged over the voxel. The corresponding results will be presented at the conference.

CONCLUSION

We have implemented the analytical integration of $\bar{\mathbf{G}}(\mathbf{r})$ over arbitrary cuboid voxel neglecting the terms of order $\mathcal{O}[(kd)^4]$. This accelerates the IGT formulation of the DDA and makes it applicable in all scenarios. It is already available in the master branch of ADDA at https://github.com/adda-team/adda, and will further be incorporated into the stable release. The improved IGT formulation leads to quadratic convergence in terms of kd for cubes, which is expected to hold for any cubically shaped scatterers as well. Also, the IGT allows robust simulation of interaction of internal sources with particles of arbitrary shape and composition.

REFERENCES

[1] Yurkin MA, Hoekstra AG. The discrete dipole approximation: an overview and recent developments. J Quant Spectrosc Radiat Transfer 2007;106:558–89.
[2] Chaumet PC, Sentenac A, Rahmani A. Coupled dipole method for scatterers with large permittivity. Phys Rev E 2004;70:036606.

[3] Smunev DA, Chaumet PC, Yurkin MA. Rectangular dipoles in the discrete dipole approximation. J Quant Spectrosc Radiat Transfer 2015;156:67–79.
[4] Yurkin MA. Performance of iterative solvers in the discrete dipole approximation. In: 2016 URSI International Symposium on Electromagnetic Theory (EMTS); 2016 Aug. 14; Espoo, Finland. IEEE Press. p. 488–91.
[5] Yurkin MA, Maltsev VP, Hoekstra AG. Convergence of the discrete dipole approximation. I. Theoretical analysis. J Opt Soc Am A 2006;23:2578–91.
[6] Wiecha PR, Majorel C, Arbouet A, Patoux A, Brûlé Y, Colas des Francs G, et al. "pyGDM" - new functionalities and major improvements to the python toolkit for nano-optics full-field simulations. Comput Phys Commun 2022;270:108142.
[7] Yurkin MA, Hoekstra AG. The discrete-dipole-approximation code ADDA: capabilities and known limitations. J Quant Spectrosc Radiat Transfer 2011;112:2234–47.
[8] Yurkin MA, Hoekstra AG. User manual for the discrete dipole approximation code ADDA 1.4.0 [Internet]. 2020 [cited 2022 Dec. 5]. Available from: https://github.com/adda-team/adda/raw/v1.4.0/doc/manual.pdf.
[9] Moskalensky AE, Yurkin MA. A point electric dipole: From basic optical properties to the fluctuation-dissipation theorem. Rev Phys 2021;6:100047.
[10] Yurkin MA, Min M, Hoekstra AG. Application of the discrete dipole approximation to very large refractive indices: Filtered coupled dipoles revived. Phys Rev E 2010;82:036703.
[11] Yurkin MA, Kahnert M. Light scattering by a cube: accuracy limits of the discrete dipole approximation and the T-matrix method. J Quant Spectrosc Radiat Transfer 2013;123:176–83.
[12] Edalatpour S, Francoeur M. The Thermal Discrete Dipole Approximation (T-DDA) for near-field radiative heat transfer simulations in three-dimensional arbitrary geometries. J Quant Spectrosc Radiat Transfer 2014;133:364–73.
[13] Rahmani A, Chaumet PC, Bryant GW. Local-field correction for an interstitial impurity in a crystal. Opt Lett 2002;27:430–2.